



UNIVERSITY OF LEEDS

This is a repository copy of *Excitation and acquisition of cranial guided waves using a concave array transducer*.

White Rose Research Online URL for this paper:  
<http://eprints.whiterose.ac.uk/140295/>

Version: Accepted Version

---

**Proceedings Paper:**

Adams, C, McLaughlan, JR [orcid.org/0000-0001-5795-4372](https://orcid.org/0000-0001-5795-4372), Nie, L [orcid.org/0000-0002-5796-907X](https://orcid.org/0000-0002-5796-907X) et al. (1 more author) (2017) Excitation and acquisition of cranial guided waves using a concave array transducer. In: Proceedings of Meetings on Acoustics. The 3rd Joint Meeting of the Acoustical Society of America and the European Acoustics Association, 25-29 Jun 2017, John B. Hynes Veterans Memorial, Boston, MA, USA. Acoustical Society of America .

<https://doi.org/10.1121/2.0000580>

---

© 2017 Acoustical Society of America. This article may be downloaded for personal use only. Any other use requires prior permission of the author and AIP Publishing. This article appeared in Adams, C, McLaughlan, JR , Nie, L et al. (1 more author) (2017) Excitation and acquisition of cranial guided waves using a concave array transducer. In: Proceedings of Meetings on Acoustics. The 3rd Joint Meeting of the Acoustical Society of America and the European Acoustics Association, 25-29 Jun 2017, John B. Hynes Veterans Memorial, Boston, MA, USA. and may be found at <http://dx.doi.org/10.1121/2>.

**Reuse**

Items deposited in White Rose Research Online are protected by copyright, with all rights reserved unless indicated otherwise. They may be downloaded and/or printed for private study, or other acts as permitted by national copyright laws. The publisher or other rights holders may allow further reproduction and re-use of the full text version. This is indicated by the licence information on the White Rose Research Online record for the item.

**Takedown**

If you consider content in White Rose Research Online to be in breach of UK law, please notify us by emailing [eprints@whiterose.ac.uk](mailto:eprints@whiterose.ac.uk) including the URL of the record and the reason for the withdrawal request.



[eprints@whiterose.ac.uk](mailto:eprints@whiterose.ac.uk)  
<https://eprints.whiterose.ac.uk/>

---

# Excitation and acquisition of cranial guided waves using a concave array transducer

Chris Adams, James McLaughlan, Luzhen Nie, Steven Freear

*Ultrasonic therapeutic transducers that consist of large numbers of unfocused, low power elements have begun to replace single, focused, high power elements. This allows the operator to use phased array techniques to change the focal position in the tissue during therapy. In transcranial therapy, this phased array configuration is essential to reduce local heating at the highly attenuating bone. Recently, Dual Mode Ultrasound Arrays (DMUAs) have been developed which leverage existing elements for imaging during therapy. DMUAs have the benefit of both the therapeutic and imaging systems being co-registered. This improves upon the existing approach of using a separate ultrasound system for guidance, as the acoustic beam path is the same for both. Unfortunately, the highly reflective nature of bone means that DMUAs have not been applied to skull imaging. However the recent near-field observation of lamb waves in cranial bone opens the possibility for DMUAs to be applied to a guided wave scan of the skull. This would allow co-registration of the bones ultrasonic properties with the therapeutic axis which would facilitate adaptive beamforming. In this work, a beamforming scheme for the excitation of guided waves in cranial bone using a therapeutic phased array is described and demonstrated experimentally.*

## 1. INTRODUCTION

Focused ultrasound has been used extensively to treat numerous diseases<sup>1-3</sup> and provide palliative care.<sup>4,5</sup> By focusing ultrasonic energy to a point using either an acoustic lens or phased array techniques,<sup>6,7</sup> tissue can be heated to ablation or to induce hyperthermia.<sup>8</sup> Researchers have begun focusing ultrasound in the brain<sup>9</sup> to ablate tissue or to modulate neurons.<sup>10,11</sup> This is made difficult however by the influence of the skull. Skull is a multi-layered hard tissue that is essential to protecting the brain of an organism. Like all bone, it is highly absorbing so when exposed to high energy sound fields it heats rapidly.<sup>12</sup> Skull is also highly attenuative<sup>13</sup> so large amounts of energy are required to achieve the desired heating at the target point. The culmination of these two properties means that the hard-soft tissue interface approaches unacceptable temperatures when exposed to high intensity focused ultrasound (HIFU).

To combat this, researchers have astutely developed new transcranial therapeutic arrays. The arrays consist of a large number of elements.<sup>14</sup> The large element count means that local tissue heating is reduced as the power is distributed across a larger area. Phased array techniques are then used to focus a beam to the target. Unfortunately, beam steering is made difficult because skull's acoustic properties vary across its entire volume. Skull consists of both cortical and trabecular layers which can vary in thickness between a wide range of values. This in turn effects the skull induced phase aberrations for each element. In order for the energy to arrive in phase at the focal point, these aberrations must be compensated for.

Compensation of the phase aberrations is achieved with a CT (computed tomography) scan using time reversal.<sup>9</sup> There are a number of downsides with this technique however. The first is that this adds a third point of failure and expense to the existing MRI and ultrasound required for therapy. It also requires exposure to harmful ionising radiation. The CT scan can only be performed before therapy and cannot compensate for patient motion or changes to the skull. Most significantly however, the CT scan is not co-registered with the therapeutic array. Small errors in the location of elements or the patient could result in artefacts in the focal region.

One obvious solution to this might be to use the therapeutic array to image the skull with ultrasound. However this is made difficult by the high attenuation of the skull bone and the limited resolution that can be achieved at non-attenuated wavelengths. Guided waves have recently been suggested as an alternative

---

---

**Table 1: Bone properties used for modelling**

Property	Symbol	Value (Cortical)	Value (Trabecular)
Density	$\rho$	1969 kg m <sup>-3</sup>	1055 kg m <sup>-3</sup>
Long. SOS	$C_L$	3476 m s <sup>-1</sup>	1886 m s <sup>-1</sup>
Shear. SOS	$C_S$	1760 m s <sup>-1</sup>	650 m s <sup>-1</sup>

ultrasonic modality for imaging the skull.<sup>15</sup>

Consisting of multiple modes of oscillation, guided waves (GW) are complex but well understood.<sup>16–19</sup> They form when a thin structure is insonified with a wavelength greater than its thickness. There are an infinite number of modes and each mode’s attenuation, group and phase velocity changes independently with frequency. Guided waves are widely used in NDT, as these distinct mode properties can be used to assess the existence of certain defects or to quantify a material’s properties. Biomechanically, they are being used to assess bone.<sup>20</sup>

Estrada et al.<sup>15</sup> have recently modelled and experimentally proven the existence of guided waves in murine skulls. Their important and pivotal work uses optoacoustic excitation and observes several guided wave modes in the near field. As an extension of this work we propose that guided waves can be observed in the far field with a phased array transducer in the concave configuration.

## 2. METHOD

We propose that many of skull’s acoustical properties can be characterised using guided waves. In this section a beam-forming technique to excite guided waves in skull using a transcranial concave array is described. The same array is used to record guided waves that leak into the water surrounding the skull. Signals are compared with known dispersion curves. Modelling parameters are given and justified herein. Minimal signal processing is required and is described at the end of this section.

### A. MODELLING

Skulls are modelled as hollow spherical shapes that change internal ( $R_1$ ) and external ( $R_2$ ) radius over their polar angles. The propagation of guided waves in spheres is complex<sup>21–24</sup> and leads to the propagation of many novel types of wave structures. Since this work concerns itself only with excitation in a 3 layer model using curved geometry transducers, skulls are modelled as cylinders that extend infinitely into the  $Z^+$  and  $Z^-$  half spaces to simplify modelling. Cylinders are used because they can be modelled in 2D space, improving simulation efficiency. Aluminium cylinders are first considered to validate the technique as the thickness can be easily adjusted, and the high velocity of sound reduced the number of computational elements. 32 different thickness cylinders between 2 and 10 mm are considered. Following this, three ply skull models are considered. Three nominal thicknesses of 3.97, 5.37 and 8.46 mm are considered. The skull consists of a trabecular layer between two layers of cortical bone. The acoustical properties are described in table 1. The skull is obtained from a CT scan of a healthy adult male. The raster CT scan is then vectorised, so that the thickness of each layer can be adjusted. The nominal radius of the inner trabecular layer and internal radius of aluminium phantoms is 87 mm. For the skulls, the percentage thickness of each layer remains constant; 35% and 29% for the cortical and trabecular layers respectively. The transducers and medium are surrounded by infinite half spaces of water as shown in figure 1.

---

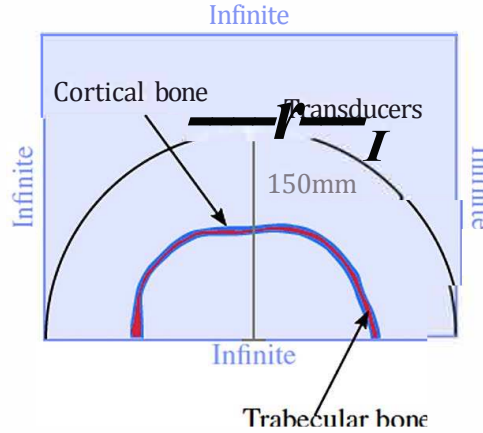


Figure 1: Simulation layout, boundaries and the 3 layer vectorised CT scan model.

## B. EXCITATION OF LEAKY MODES

To excite lamb waves in the media, plane waves are generated so that they are obliquely incident on the media. Experimentally, it was found that an incidence angle of  $60^\circ$  is effective at exciting lamb modes in ex-vivo skull. The curved geometry of the therapeutic array means that the angle of incidence is not the same as the plane wave steering angle. The relationship between the two is depicted in figure 2. Here the blue shape represents a cross section of a skull, and point  $P$  is chosen to be insonified. To achieve the desired angle of incidence, a number of elements are selected from angle  $\phi$  with a width of  $d$ . The elements generate a plane wave at an angle  $\theta$ . The distances from the transducers and from point  $P$  to the geometric centre are  $R_2$  and  $R_1$  respectively. To calculate  $\phi$  the following equation is used:

$$\phi = \theta - \sin^{-1} \left( \frac{R_1 \sin(\theta)}{R_2} \right) \quad (1)$$

Once  $\phi$  is known, the steering angle  $\theta$  can be calculated with the following:

$$\theta = \phi + \sin^{-1} \left( \frac{R_1 \sin(\phi)}{R_2} \right) \quad (2)$$

Elements within a bounding box of width  $d$  are used to generate the plane wave. To calculate the delays for each element, the cartesian grid is first rotated about the transducer geometric centre and then again by the co-ordinates of the edge element:

$$C = [B \cdot \cos(\theta) - A \cdot \sin(\theta); B \cdot \sin(\theta) + A \cdot \cos(\theta)] \quad (3)$$

Here,  $B$  represents the selected elements' Cartesian co-ordinates.  $A$  is a vector containing the edge co-ordinates and is subtracted column-wise ( $p$ ) from the rotated  $B$  co-ordinates. This is so the subsequent rotation of  $C$  is performed around the edge element. The  $y$  co-ordinates of  $C$  now equal the distance to an imaginary plane at an angle  $\theta$  to the elements. These distances  $y$  can be used to calculate the correct delays.

The transducer consists of 128 pressure loads distributed evenly between 0 and  $\pi$  radians. The nominal convex radius of 150 mm is increased by the thickness of the aluminium cylinder and half the thickness of the skull. This is such that the distance between the surface and transducer remains constant between simulations. AU selected transmitting elements are excited with a blakman-harris shaped wavelet. A hamming window is applied to reduce side lobes. For the aluminium models, the centre frequency is 200 kHz, for the skull models, 67 kHz is used. Figure 4 shows the range  $[a - b]$  of frequency-thickness products that can be considered using this frequency. In this range, the changes in group velocity of the  $F(1, 1)$  and  $F(1, 3)$

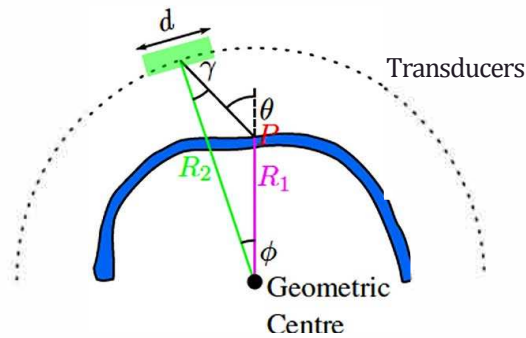


**Figure 2: Geometry of simulation, the blue represents the vectorised skull shape and the dashes represent the transducers. The correct transmitting transducers must be selected from the array to achieve the desired angle of incidence**

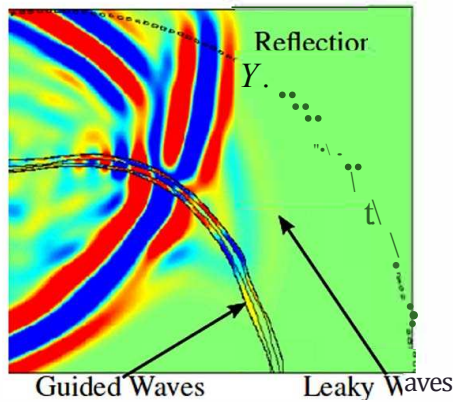


**Figure 3: Snapshot from the simulation that demonstrates that three layer skull models can host guided waves. Energy from these guided waves leak into the surrounding fluid.**

modes should be visible. Similarly, figure 5 also shows the group velocity for the first order flexural modes, the three considered  $fd$  products are shown with red lines.

### C. SIGNAL ACQUISITION

The majority of the energy in the field of view will consist of bulk reflection from the boundary between the water and medium. As the faster guided waves move around the cylinder however, it becomes easier to separate the leaking energy from the reflection. For this reason an arbitrary transducer in the array some small angle from the insonified area is chosen to acquire the signals. A large angle makes temporal windowing easier as the leaking waves are more separated from the reflection energy, this however introduces averaging effects. Conversely, a small angle makes windowing more difficult but provides more localised information about acoustic properties. In simulations, a liberal value of  $70^\circ$  has been used. Figure 6 shows a snapshot from a simulation and demonstrates how after a small amount of time the higher velocity guided waves can be separated from the reflected energy (figure 3). Once windowing has taken place the signal undergoes the Hilbert transform to extract its envelope.

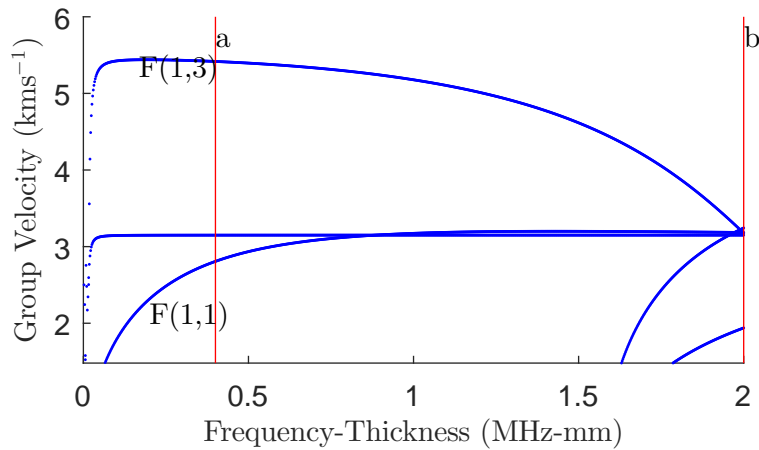


**Figure 4:** The group velocity of the first order flexural modes in an aluminium cylinder. The red lines show the range of thicknesses that are considered.

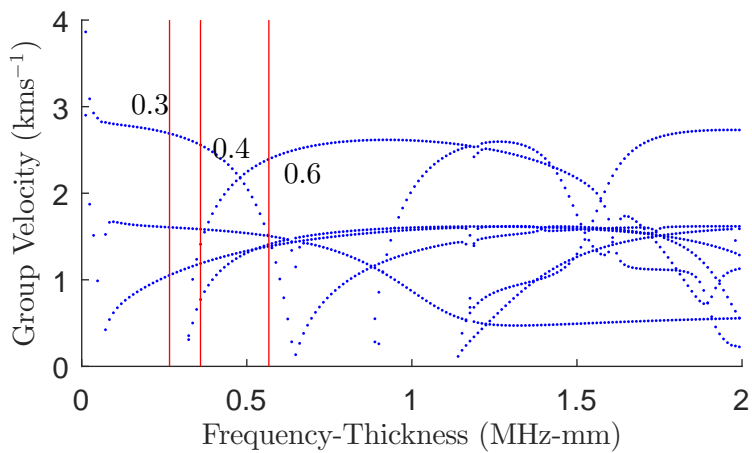


**Figure 5:** The group velocity of first order flexural modes in a three layer skull cylinder. The red lines show the three different thicknesses of skulls that are considered.

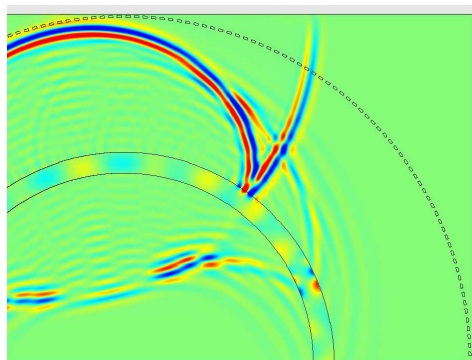


**Figure 6:** Snapshot from the simulation of the aluminium model. It shows Guided modes travel faster than the reflected energy in an aluminium cylinder.

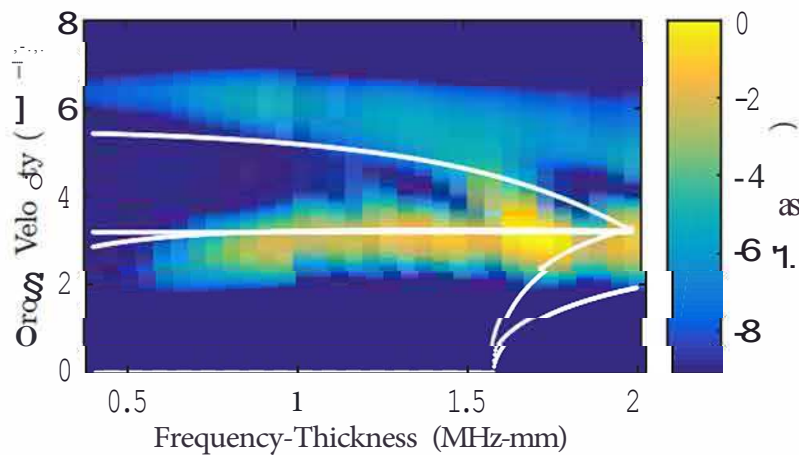


**Figure 7:** The group velocity of leaking modes changes with thickness. There is a small difference between theoretical predictions and measured results

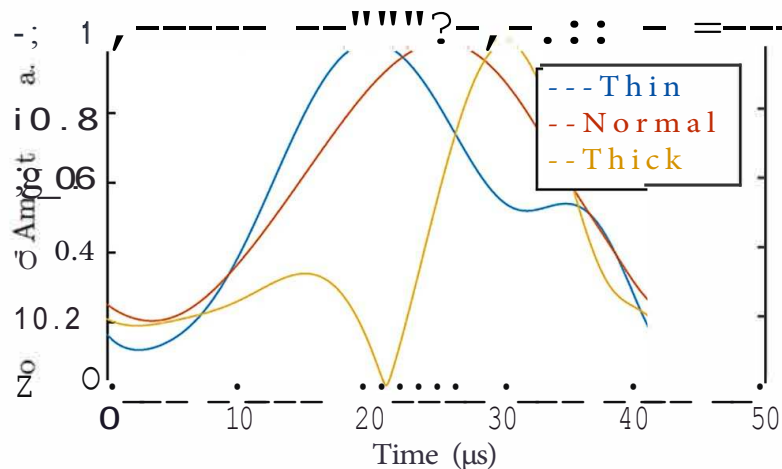


**Figure 8:** The envelopes of recorded windowed signals indicate a change in velocity as skull thickness changes

### 3. RESULTS AND DISCUSSION

Figure 7 shows the signal envelopes for different thickness of cylinders. Once propagation time is subtracted, the amalgamation of the signal envelopes can be presented as a graph of group velocities related to frequency-thickness. The intensity represents power, with the maximum amplitude used as a reference. In white, the theoretical group velocity is overlaid. There is some disagreement between the simulation and theoretical results, particularly for the mode  $F(1, 2)$ . This is likely because the fluid loading is not taken into consideration. To compound this, wave shapes for both modes at two points on the dispersion curves are presented in figure 9. It can be seen that mode  $F(1, 2)$  has low radial and circumferential displacements which may change along with velocity when fluid loading is introduced.

Figure 8 shows the envelopes for captured waveforms from the three different thicknesses of skulls. Blue, red and gold represent 3.97, 5.37 and 8.46 mm respectively. As thickness increases so does the time of arrival. This is indicative of a reduction in velocity as the distance between experiments is maintained. When figure 5 is considered, a reduction in speed of the fastest mode  $F(1, 3)$  is expected with these experimental parameters.

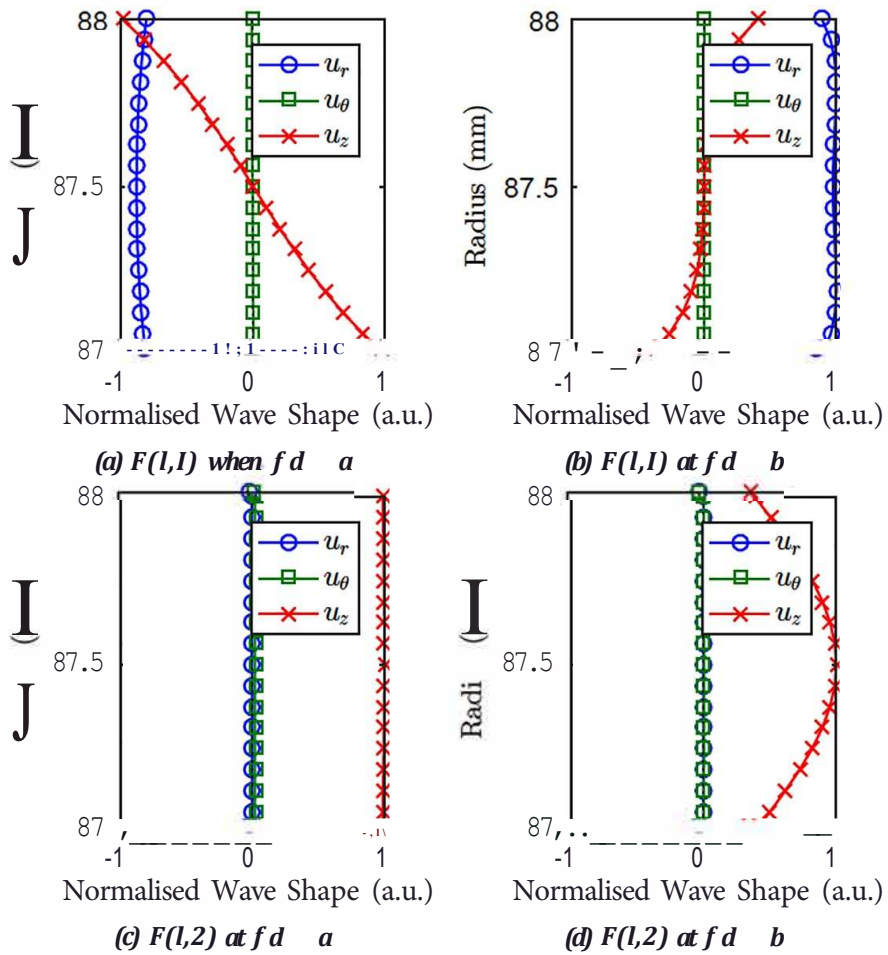


Figure 9: Wave shape changes according to frequency and mode.  $U_r$  is displacement in the radius,  $U_z$  is displacement along the length of the cylinder,  $u_\theta$  is displacement in the circumference

---

The results show that it is possible to excite guided waves in a three layered skull model using an unconventional geometry. It was also shown that the nominal thickness has an impact on the velocity of these guided waves.

A number of simplifications were made modelling. Firstly, a cross section of skull was modelled instead of a full 3D model, this reduced the number of computational elements by a factor of 1520. This work concerned itself primarily with the challenge of exciting guided waves in a curved skull model with a concave transducer, which has been shown. However further modelling should be conducted to determine the influence of the skull shape and artefacts on measurements. With respect to array modelling, 128 elements were chosen, which is perhaps denser than clinical systems where 1024 elements are used to cover the whole skull. To aid simulation performance, frequencies lower than what is clinically available were used. Experimentally, increasing the excitation frequency and reducing the element density will induce grating and side lobes. It will also mean that the generated plane wave needs more distance to form. This should not prove to be problematic however as the angle of incidence is not particularly critical and only the part of the wave front at the correct angle will propagate into guided waves anyway.

Further mathematical analysis should be conducted with respect to mode propagation. The influence of overall speed of sound with respect to individual layers should be considered. Dispersion curves for a fluid loaded 3 layer skull should also be calculated. This would allow a measured arrival time to be converted to specific layer properties.

There is much scope for signal processing development, the most important would be the introduction of tomography. A full 3D system would allow plane waves to insonify the skull at numerous locations at multiple directions. Tomography could then be used to calculate localised changes to skull properties. This could be used to generate a thorough map of thickness change that is co-located to the therapeutic array. This should be supplemented with a technique to better separate bulk reflection from leaked guided wave energy. Currently, signals are separated temporally which means receiving elements must be chosen some distance away from the transmitters to allow the faster waves to separate. The means to extract the guided waves from signals that are superimposed with the reflection means the receiver could be placed closer and thus would reduce averaging effects.

## 4. CONCLUSION

The non invasive nature of focused ultrasound is making it an increasingly popular surgical tool. It is rapidly gaining traction in transcutaneous neuro modulation and ablation of brain tissue. To perform transcranial therapy however, an MRI is required in addition to a CT scan. The CT scan is required to compensate for skull-induced phase aberrations which vary across its volume. There are some downsides to this, such as the exposure to harmful ionising radiation which should be avoided. Additionally the CT scan is not co-registered with the therapeutic transducers which might cause an error in the focal position. Ultrasound imaging could be used as an alternative, but this is made difficult by high attenuation and low resolution offered at large wavelengths. Investigators have already suggested guided waves as an alternate ultrasonic technique for inspecting the skull. Their work involves characterisation of guided waves in murine skulls in the near field using opto-acoustic excitation. Here, it was proposed that these guided waves could also be observed in the far field using a concave geometry transducer. This would facilitate quantification of localised changes in skull acoustic properties to be quantified in a way that was co-located with the therapeutic array. A number of modelling simplifications were made and justified, such as using cylinders instead of spheres. A scheme for generating guided waves in skull is described. The proposed technique consists of three stages. The first involves selecting the area of skull to be inspected. The second involves choosing a number of elements from the array to achieve the required angle of incidence tangential to the skull. Finally, delays are applied to a wavelet excitation to produce an angled plane wave. The obliquely incident waves interact with the skull to produce guided waves. In order to separate the guided waves

---

---

from reflected spectra, temporal windowing is used, followed by a Hilbert transform to estimate the group velocity. A number of different thickness aluminium models were considered along with 3 thicknesses of skulls. Measurements from the aluminium models were compared with theoretical dispersion curves and exhibited the expected behaviour with respect to changes in velocity. However, there was some disagreement in the exact value, likely due to the effects of water loading which was not considered. In skull, a decrease in velocity with increase in thickness was observed which was expected. Further efforts should be focused on signal processing and modelling to improve accuracy, better understand the effects of fluid loading and to select more appropriate modes.

## REFERENCES

- <sup>1</sup> Gail Ter Haar. Therapeutic applications of ultrasound. *Progress in biophysics and molecular biology*, 93(1):111–129, 2007.
  - <sup>2</sup> Kevin D Evans, Brandon Weiss, and Michael Knopp. High-intensity focused ultrasound (hifu) for specific therapeutic treatments: a literature review. *Journal of Diagnostic Medical Sonography*, 23(6):319–327, 2007.
  - <sup>3</sup> RO Illing, JE Kennedy, F Wu, GR Ter Haar, AS Protheroe, PJ Friend, FV Gleeson, DW Cranston, RR Phillips, and MR Middleton. The safety and feasibility of extracorporeal high-intensity focused ultrasound (hifu) for the treatment of liver and kidney tumours in a western population. *British journal of cancer*, 93(8):890, 2005.
  - <sup>4</sup> Merel Huisman, Gail Ter Haar, Alessandro Napoli, Arik Hananel, Pejman Ghanouni, György Lövey, Robbert J Nijenhuis, Maurice AAJ Van Den Bosch, Viola Rieke, Sharmila Majumdar, et al. International consensus on use of focused ultrasound for painful bone metastases: Current status and future directions. *International Journal of Hyperthermia*, 31(3):251–259, 2015.
  - <sup>5</sup> D Bianchini, F Marocci, E Menghi, V DErrico, E Mezzenga, and A Sarnelli. Treatment plan verification in mrgfus for bone metastasis pain palliation. *Physica Medica: European Journal of Medical Physics*, 32:248, 2016.
  - <sup>6</sup> R Seip, W Chen, J Tavakkoli, LA Frizzell, and NT Sanghvi. High-intensity focused ultrasound (hifu) phased arrays: Recent developments in transrectal transducers and driving electronics design. In *Proc. 3rd Int. Symp. on Therapeutic Ultrasound*, pages 423–428, 2003.
  - <sup>7</sup> P Smirnov and K Hynynen. Design of a hifu array for the treatment of deep venous thrombosis: a simulation study. *Physics in medicine and biology*, 2017.
  - <sup>8</sup> Ari Partanen, Pavel S Yarmolenko, Antti Viitala, Sunil Appanaboyina, Dieter Haemmerich, Ashish Ranjan, Genevieve Jacobs, David Woods, Julia Enholm, Bradford J Wood, et al. Mild hyperthermia with magnetic resonance-guided high-intensity focused ultrasound for applications in drug delivery. *International journal of hyperthermia*, 28(4):320–336, 2012.
  - <sup>9</sup> Mathieu Pernot, Jean-Francois Aubry, Mickael Tanter, Anne-Laure Boch, Fabrice Marquet, Michele Kujas, Danielle Seilhean, and Mathias Fink. In vivo transcranial brain surgery with an ultrasonic time reversal mirror. *Journal of neurosurgery*, 106(6):1061–1066, 2007.
  - <sup>10</sup> Joseph Blackmore, Michele Veldsman, Christopher Butler, and Robin Cleveland. Focusing ultrasound through the skull for neuromodulation. *The Journal of the Acoustical Society of America*, 141(5):3549–3549, 2017.
-

- 
- <sup>11</sup> Omer Naor, Steve Krupa, and Shy Shoham. Ultrasonic neuromodulation. *Journal of neural engineering*, 13(3):031003, 2016.
- <sup>12</sup> Christopher W Connor and Kullervo Hynynen. Patterns of thermal deposition in the skull during transcranial focused ultrasound surgery. *IEEE transactions on biomedical engineering*, 51(10):1693–1706, 2004.
- <sup>13</sup> Gianmarco Pinton, Jean-Francois Aubry, Emmanuel Bossy, Marie Muller, Mathieu Pernot, and Mickael Tanter. Attenuation, scattering, and absorption of ultrasound in the skull bone. *Medical physics*, 39(1):299–307, 2012.
- <sup>14</sup> Mathieu Pernot, Jean-François Aubry, Mickaël Tanter, Jean-Louis Thomas, and Mathias Fink. High power transcranial beam steering for ultrasonic brain therapy. *Physics in medicine and biology*, 48(16):2577, 2003.
- <sup>15</sup> Héctor Estrada, Johannes Rebling, and Daniel Razansky. Prediction and near-field observation of skull-guided acoustic waves. *Physics in Medicine and Biology*, 62:4728, 2017.
- <sup>16</sup> Chris Adams, Sevan Harput, David Cowell, Thomas M Carpenter, David M Charutz, and Steven Freear. An adaptive array excitation scheme for the unidirectional enhancement of guided waves. *IEEE transactions on ultrasonics, ferroelectrics, and frequency control*, 64(2):441–451, 2017.
- <sup>17</sup> Chris Adams, James R McLaughlan, Luzhen Nie, David Cowell, Thomas Carpenter, and Steven Freear. Excitation of leaky lamb waves in cranial bone using a phased array transducer in a concave therapeutic configuration. *The Journal of the Acoustical Society of America*, 2017.
- <sup>18</sup> Chris Adams, Sevan Harput, David Cowell, Steven Freear, and David M Charutz. Specimen-agnostic guided wave inspection using recursive feedback. In *Ultrasonics Symposium (IUS), 2016 IEEE International*, pages 1–4. IEEE, 2016.
- <sup>19</sup> Chris Adams, Sevan Harput, David Cowell, and Steven Freear. A phase velocity filter for the measurement of lamb wave dispersion. In *Ultrasonics Symposium (IUS), 2016 IEEE International*, pages 1–4. IEEE, 2016.
- <sup>20</sup> Nicolas Bochud, Quentin Vallet, Jean-Gabriel Minonzio, and Pascal Laugier. Predicting bone strength with ultrasonic guided waves. *Scientific Reports*, 7:43628, 2017.
- <sup>21</sup> Song Qiao, Xinchun Shang, and Ernian Pan. Elastic guided waves in a coated spherical shell. *Nondestructive Testing and Evaluation*, 31(2):165–190, 2016.
- <sup>22</sup> Andrew N Norris and AL Shuvalov. Elastodynamics of radially inhomogeneous spherically anisotropic elastic materials in the stroh formalism. In *Proc. R. Soc. A*, volume 468, pages 467–484. The Royal Society, 2012.
- <sup>23</sup> Jianmin Qu, Yves Berthelot, and Zhongbo Li. Dispersion of guided circumferential waves in a circular annulus. 1996.
- <sup>24</sup> GC Gaunaurd and MF Werby. Similarities between various lamb waves in submerged spherical shells, and rayleigh waves in elastic spheres and flat half-spaces. *The Journal of the Acoustical Society of America*, 89(6):2731–2739, 1991.
-